AN INCLUSIVE VIEW ON $\bar{p}p \to n\pi$ AT REST

CERN - Collège de France Collaboration
(Presented by C. Ghesquière)

In the phenomenological analysis of high energy interactions, one is led to attempt to fit the data by means of what is currently known as the intermediate cluster model.

It turns out that the mean energy and mean multiplicity of the clusters, when fitted over the results, appears to be very close of the values found for $\bar{p}p$ annihilation at rest: $\langle E \rangle \approx 2$ GeV and $\langle n_\pi \rangle \approx 4$.

This led us to deduce from the annihilation at rest some properties that could may be thrown in the model and give some insight in the field of high energy interactions.

In a first step we wanted to convince ourselves that it was worth to consider that hypothesis further and we choosed to compare the single particle inclusive spectra $d\sigma/dp_T$ in $\bar{p}p$ at rest on one side, in clusters on the other side.

For $\bar{p}p$ at rest we have used the results of older measurements amounting to

37799 2 prong events
57652 4 prong events
2127 6 prong events

8 prongs are neglibible.

Some weighting was done in order to correct for measurement biases mainly due to tracks interacting or decaying inside the chamber. The normalisation of the channels was done according to the scanning rates shown in table 1.

TABLE 1

Prong	Scanning Rates
0	$(4.1\ ^{+\ 0.2}_{-\ 0.6})\ 10^{-2}$
2	$(43.2\ ^{+\ 0.9}_{-\ 0.7})\ 10^{-2}$
4	$(48.6\ ^{+\ 0.9}_{-\ 0.7})\ 10^{-2}$
6	$(4.1\ ^{+\ 0.2}_{-\ 0.2})\ 10^{-2}$

In order to get the inclusive spectrum $d\sigma/dp_T$ we projected over an arbitrary axis in space as the annihilations show a complete spherical symmetry in space and added a $\frac{1}{\cos \Theta}$ correction to simulate the slicing in X which is currently applied to get the distribution in high energy interactions.

The results in $d\sigma/dp_T$, $d\sigma/dp_T^2$ and $E^* d\sigma/dp_T^2$ which are currently used in the litterature are displayed both in table 2 and in Fig. 1.2. The units are arbitrary

TABLE 2

P_T GeV/c	dn/dp_T	P_T^2 $(GeV/c)^2$	dn/dp_T^2	$E^* dn/dp_T^2$
0.05	200 ± 2	0.005	10.2 ± 0.01	1.56
0.15	540 ± 3	0.025	9 ± 0.05	1.80
0.25	563 ± 3	0.065	5.64 ± 0.03	1.64
0.35	392 ± 2	0.125	2.86 ± 0.025	1.09
0.45	228 ± 1.1	0.205	1.25 ± 0.02	0.590
0.55	117 ± 1.1	0.305	0.54 ± 0.01	0.315
0.65	62 ± 0.9	0.425	0.24 ± 0.005	0.160
0.75	36 ± 0.8	0.565	0.15 ± 0.002	0.087
0.85	18 ± 0.7	0.725	0.050± 0.002	0.042

To be representative of the emission of clusters we took the distribution $d\sigma/dp_T$ or equivalently $d\sigma/dp_T^2$ of pions, at $X = \frac{2P_L}{\sqrt{s}}$, close to 0, at s as high as possible and for reactions where the emitted pion is of different nature than both the beam and the target.

The reactions used for comparison are listed below

$\bar{p}p \to \pi^+$ ... at 2.23 GeV/c Ref. 1 - Fig. 3-4

$\pi^+ p \to \pi^-$ ... at 18.5 GeV/c Ref. 2 - Fig. 5-6

$pp \to \pi^-$ ... at 28.5 GeV/c Ref. 3 - Fig. 7

$pp \to \pi^\pm$ ... up to 1500 GeV/c Ref. 4 - Fig. 8

$\gamma^- p \to \pi^-$ ... at 9.3 GeV/c Ref. 5 - Fig. 9

The curves drawn on the figures correspond to $\bar{p}p$ annihilations at rest.

Although at first glance the agreement may look perfect but for the cut-off at high momenta due to phase space, a closer look reveals that at very low P_T the $\bar{p}p$ data are systematically lower than for other reactions. This effect disappears at intermediate value of X (X $\simeq$ 0.1 to 0.3) showing that some experimental effect may cause this systematic behaviour.

Nevertheless, we feel that the agreement is good enough and that we can deduce some more useful inclusive informations from our $\bar{p}$. As an example we can take the multiplicities.

1) Charged prong multiplicities:

From the table 1, one can deduce

$$\langle n_{ch} \rangle = 3.054 \begin{matrix} + 0.040 \\ - 0.036 \end{matrix}$$

$$D^2_{ch} = \langle n^2_{ch} \rangle - \langle n_{ch} \rangle^2 = 1.653$$

$$\frac{\langle n_{ch} \rangle}{D_{ch}} = 2.37,$$

A result close to the KNO scaling value.

2) Total π multiplicity.

The individual multineutral contributions have been evaluated by fitting the histograms from the involved channels with superposition of multineutrals calculated with adhoc matrix elements. For instance the $\bar{p}p \to \pi^+\pi^-$ (missing mass) have been evaluated through the following states

$4\pi \to \rho^+_o\pi^-_o\pi^o$, $\rho^+\rho^-$, $\rho^o f^o$, phase space

$5\pi \to \rho^+_o\pi^-_o\pi^o\pi^o$, $\rho^+\rho^-\pi^o$, $\eta\pi^+\pi^-$, $\omega\pi^o\pi^o$, phase space

$6\pi \to \rho^+_o\pi^-_o\pi^o\pi^o\pi^o$, phase space

$7\pi \to \rho^+_o\pi^-_o\pi^o\pi^o\pi^o\pi^o$, $\omega\pi^o\pi^o\pi^o\pi^o\pi^o$, phase space,

the contribution of some of these states being deduced from the fitted channels, for instance $\rho^o f^o$ can be obtained from the $\bar{p}p \to \pi^+\pi^+\pi^-\pi^-$ ... The 0 prong final state deserves a special treatment and the counterpart contribution from the various charged states have been deduced as much as we can do by isospin coupling.

The general result is summarized in Table 3 giving the topological channels.

TABLE 3

Channel	Rate/annihilation (X 10^2)	Channel	Rate/annihilation (X 10^2)
$\pi^+\pi^-$			0.375 ± 0.030
$\pi^+\pi^-\pi^o$			6.9 ± 0.35
		$\pi^+\pi^-\pi^o\pi^o$	9.3 ± 3.0
$\pi^+\pi^- x^o$	35.8 ± 0.8 →	$\pi^+\pi^-\pi^o\pi^o\pi^o$	23.3 ± 3.0
		$\pi^+\pi^-\pi^o\pi^o\pi^o\pi^o$	2.8 ± 0.7

TABLE 3 (Cont'd)

Channel	Rate/annihilation (x 10^2)	Channel	Rate/annihilation (x 10^2)
$\pi^+\pi^+\pi^-\pi^-$			6.9 ± 0.6
$\pi^+\pi^+\pi^-\pi^-\pi^o$			19.6 ± 0.7
$\pi^+\pi^+\pi^-\pi^-X^o$	20.8 ± 0.7 →	$\pi^+\pi^+\pi^-\pi^-\pi^o\pi^o$	16.6 ± 1.
		$\pi^+\pi^+\pi^-\pi^-\pi^o\pi^o\pi^o$	4.2 ± 1.
$\pi^+\pi^+\pi^+\pi^-\pi^-\pi^-$			2.1 ± 0.25
$\pi^+\pi^+\pi^+\pi^-\pi^-\pi^-\pi^o$			1.85± 0.15
$\pi^+\pi^+\pi^+\pi^-\pi^-\pi^-X^o$		$\pi^+\pi^+\pi^+\pi^-\pi^-\pi^-\pi^o\pi^o$	0.3 ± 0.1

From this table a total prong mutliplicity distribution is obtained in Table 4.

TABLE 4

n_π	Frequency (x10^2)
2	0.38 ± 0.03
3	7.8 ± 0.4
4	17.5 ± 3.0
5	45.8 ± 3.0
6	22.1 ± 1.5
7	6.1 ± 1.
8	0.3 ± 0.1

Then it appears that

$$\langle n_\pi \rangle = 5.01 \pm 0.23$$

$$D_\pi^2 = \langle n_\pi^2 \rangle - \langle n_\pi \rangle^2 = 1.04$$

$$\frac{\langle n_\pi \rangle}{D_\pi} = 4.1$$

The distribution is very sharply peaked at 5. and narrow.

3) Total π^o number:

From Table 3 one also deduces the relative frequency

$$n_{\pi^\pm}/_{\text{annihilation}} = 1.53$$

$$n_{\pi^o}/_{\text{annihilation}} = 1.96\ (\pm 0.23)$$

showing that there is an excess of π^o that we can express either as

$$n_{\pi o} = n_{\pi^\pm} + 0.44\ (\pm\ 0.23)$$

or

$$\frac{n_{\pi o}}{n_{\pi^\pm}} = 1.27\ (\pm\ 0.14)$$

π^o spectrum:

The process of fitting the histograms is too crude to allow us to deduce a spectrum of π^o. The only thing we can calculate is from the average momentum (Energy) of charged pions, which turns to be $\langle p_{ch} \rangle = 0.345$ GeV/c $\langle E_{ch} \rangle = 0.374$ GeV the average π^o momentum

$$\langle P_o \rangle = 0.352 \text{ GeV/c}$$

which is equal to the average momentum for the charged pions within errors.

More information can be gained from the $\bar{p}$ at rest, for instance in the field of two particle correlations, and may be usefully applied to clusters decays, but as there exist no method to isolate the decay products of a cluster from the neighbour products, the comparison will remain indirect and probably not too convincing.

REFERENCES

1) Inclusive $\bar{p} + p \to \pi$ + anything at 2.23 GeV/c.
T.F. Hoang, D. Rhines and W.A. Cooper P.R.L. 27 (1971) p. 1681.

2) Longitudinal and transverse momentum distribution for π^- mesons in 18.5 GeV/c $\pi^\pm p$ interactions.
N.N. Biswas, N.M. Cason, V.P. Kenney, J.T. Powers, W.D. Shephard and D.W. Thomas.
P.R.L. 26 (1971) p.1589.

3) Pion spectra from the reactions $pp \to \pi^\pm$ anything at 28.5 HeV.
W.H. Sims, J. Hanlon, E.O. Salant, R.S. Panvini, R.R. Kinsey, T.W. Morris and L. Von Lindern.
N.P. B41 (1972) p.317.

4) Charged particle production at 90^o in the center of mass in very high energy proton-proton collisions.
M. Banner, J.L. Hamel, J.P. Pansart, A.V. Stirling, J. Teiger, H. Zaccone, J. Zsembery, G. Bassompierre, M. Croissiaux, J. Gresser, R. Morand, M. Riedinger and M. Schneegans.
P.L. 41B (1972) p.547.

5) A study of the inclusive reactions $\gamma p \to \pi^-$ + (anything) with polarized photons at 2.8, 4.7 and 9.3 GeV.
K.C. Moffeit, J. Ballam, G.B. Chadwick, M. Della Negra, R. Gearhart, J.J. Murray, P. Seyboth, C.K. Sinclair, I.O. Skillicorn, H. Spitzer, G. Wolf, W.H. Bingham, W.B. Fretter, W.J. Podolsky, M.S. Rabin, A.H. Rosenfeld, R. Windmolders and G.P. Yost.
P.R. D5 (1972) p.1603.

FIGURE CAPTIONS

1) Distribution of dN/dP_T for $\bar{p}$ stop obtained by projecting dN/dP on an arbitrary axis. The curve is not the result of a fit but is hand drawn to guide to eye. This curve will be used when comparing the spectrum with other data.

2) Experimental distribution of dN/dP_T^2 for $\bar{p}$, (full line), obtained from the preceeding distribution dN/dP_T and distribution $E^* dN/dP_T^2$ (dotted line).

3) Experimental distribution $\frac{d^2\sigma}{dP_T^2\, dP_L}$ for $\bar{p}p$ at 2.23 GeV/c (ref. 8). The points at rest are superposed as crosses.

4) Experimental distribution $\langle p_T \rangle$ as a function of $|p_L|$ for 2.23 GeV/c $\bar{p}p$. The point at rest is shown as a cross at $p_L = 0$.

5) Experimental $\frac{d^2\sigma}{dQ^2}$ for $\pi^+ p \to \pi^- X$ at 18.5 GeV/c, $Q^2 = p_T^2$, for various X. The $\bar{p}$ distribution is schematrized by the full line curve.

6) Experimental distribution $d\sigma/dQ$ for $\pi^+ p \to \pi^- X$ at 18.5 GeV/c (ref. 9) $Q = p_T$. The $\bar{p}$ distributions are shown as dotted lines on the two distributions $0 < x < 0.04$ and $0.04 < x < 0.1$.

7) Experimental distribution $d\sigma/dp_T^2$ for $pp \to \pi^- x$ at 28.5 GeV/c (ref. 10) for various Y. The $\bar{p}$ distribution is shown as a dotted line curve on the distribution $0 < Y < 0.2$.

8) Experimental distribution $E^* \frac{d\sigma}{dp_T^2}$ for $pp \to \pi^- X$ at ISR energies (ref. 11) at various X. The $\bar{p}$ distribution $\frac{d\sigma}{dp_T^2}$ is represented by the full line curve.

9) Experimental distribution $\frac{1}{\pi} \frac{E}{p_{max}} \frac{\Delta\sigma}{\Delta p_T^2}$ for $\gamma p \to \pi^- X$ at 9.3 GeV (ref. 12) and various X. The $\bar{p}$ data $E^* \frac{dN}{dp_T^2}$ is shown as full line curve.

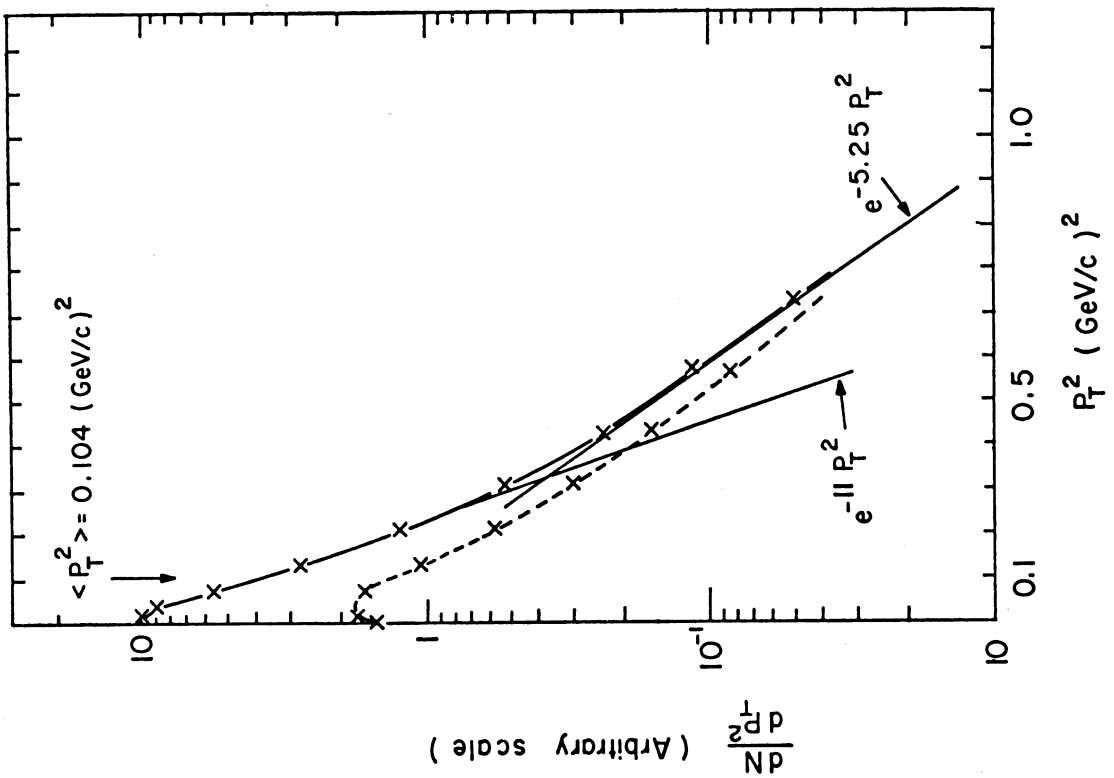
$\frac{dN}{dP_T^2}$ (Arbitrary scale)
P_T^2 (GeV/c)^2
$<P_T^2>$ = 0.104 (GeV/c)^2
$e^{-5.25\ P_T^2}$
$e^{-11\ P_T^2}$

Fig. 2

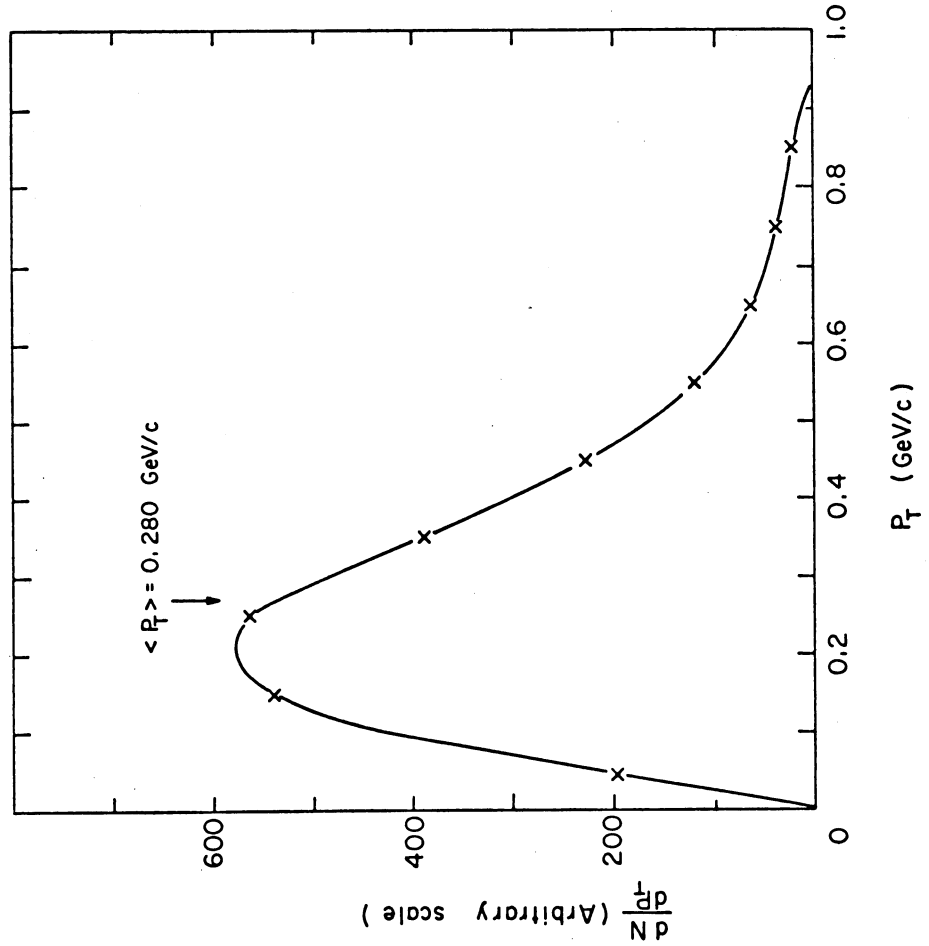
$\frac{dN}{dP_T}$ (Arbitrary scale)
P_T (GeV/c)
$<P_T>$ = 0.280 GeV/c

Fig. 1

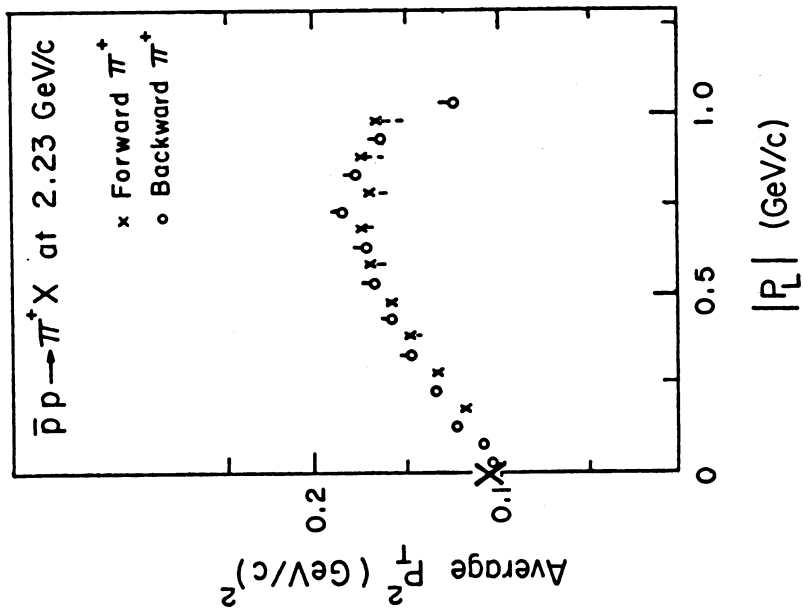
$\bar{p}p \to \pi^+ X$ at 2.23 GeV/c
× Forward π^+
○ Backward π^+
Average P_T^2 $(GeV/c)^2$
0.2
0.1
0
0.5
1.0
$|P_L|$ (GeV/c)

Fig. 4

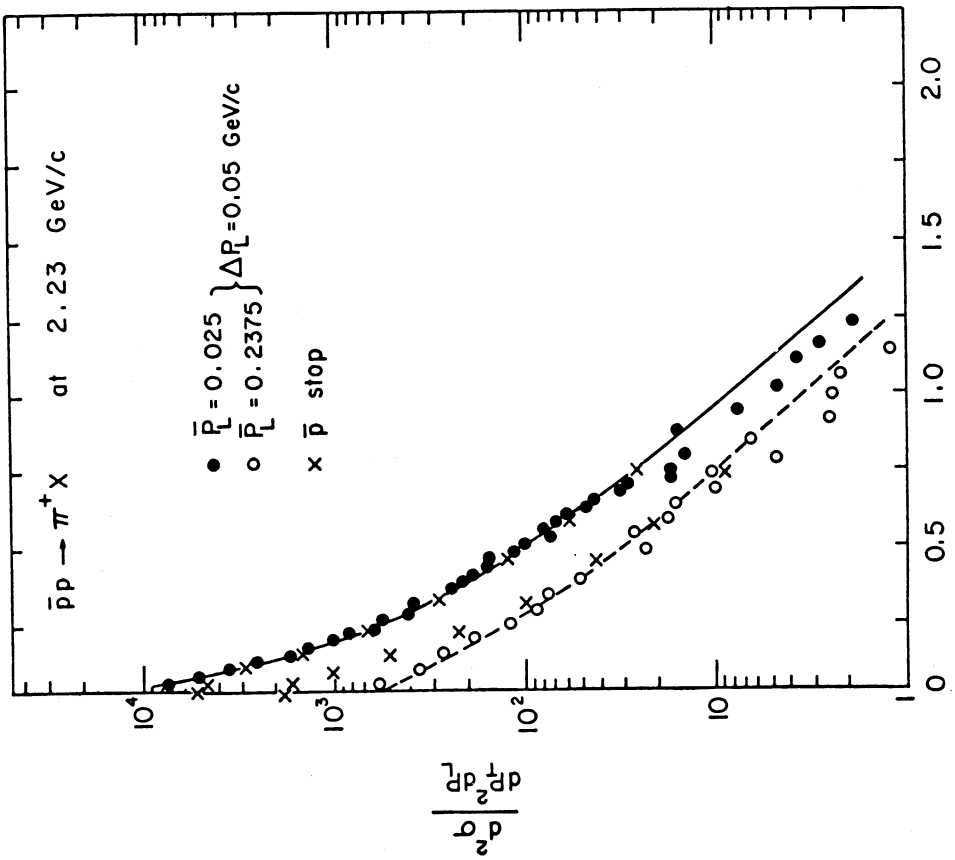
$\bar{p}p \to \pi^+ X$ at 2.23 GeV/c
● $\bar{P}_L$ = 0.025
○ $\bar{P}_L$ = 0.2375
} ΔP_L = 0.05 GeV/c
× $\bar{p}$ stop
$\frac{d^2\sigma}{dP_T^2 dP_L}$
10^4
10^3
10^2
10
1
0
0.5
1.0
1.5
2.0
P_T^2 $(GeV/c)^2$

Fig. 3

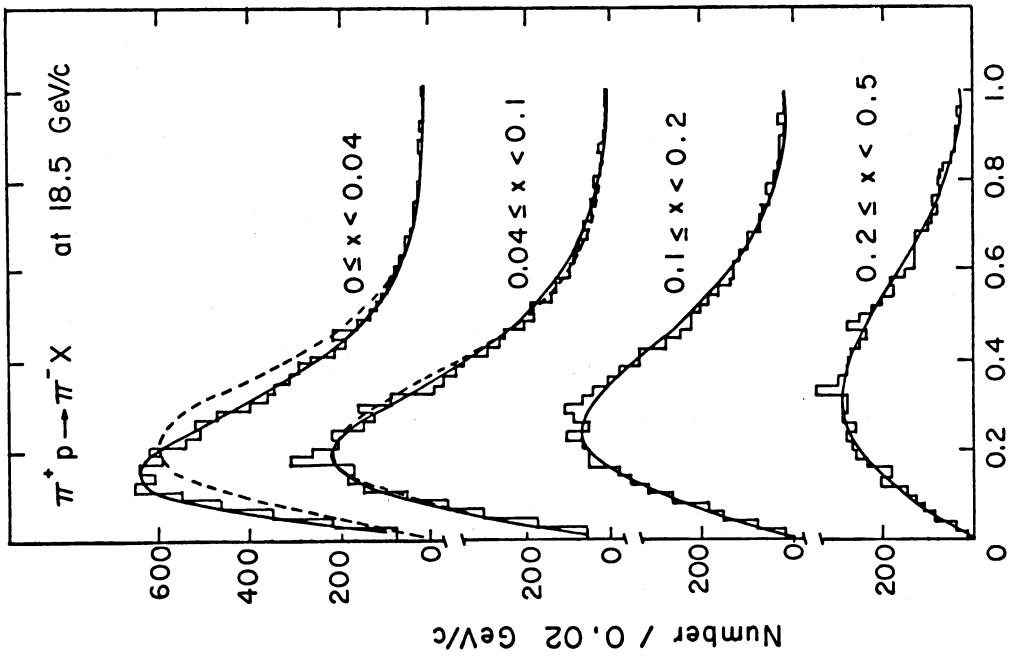
$\pi^+ p \to \pi^- X$ at 18.5 GeV/c
$0 \le x < 0.04$
$0.04 \le x < 0.1$
$0.1 \le x < 0.2$
$0.2 \le x < 0.5$
Number / 0.02 GeV/c
Q (GeV/c)

Fig. 6

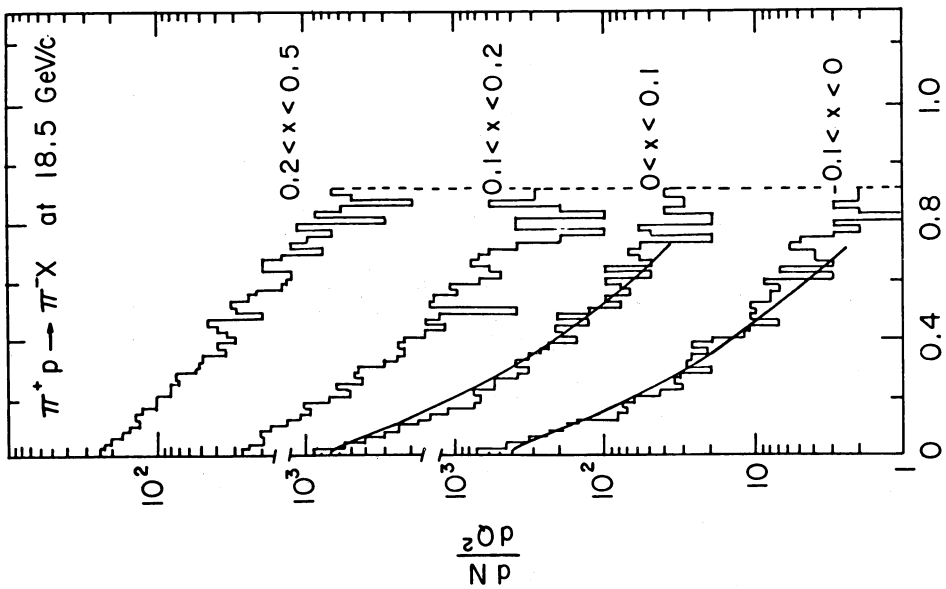
$\pi^+ p \to \pi^- X$ at 18.5 GeV/c
$0.2 < x < 0.5$
$0.1 < x < 0.2$
$0 < x < 0.1$
$-0.1 < x < 0$
$\frac{dN}{dQ^2}$
Q^2 (GeV/c)^2

Fig. 5

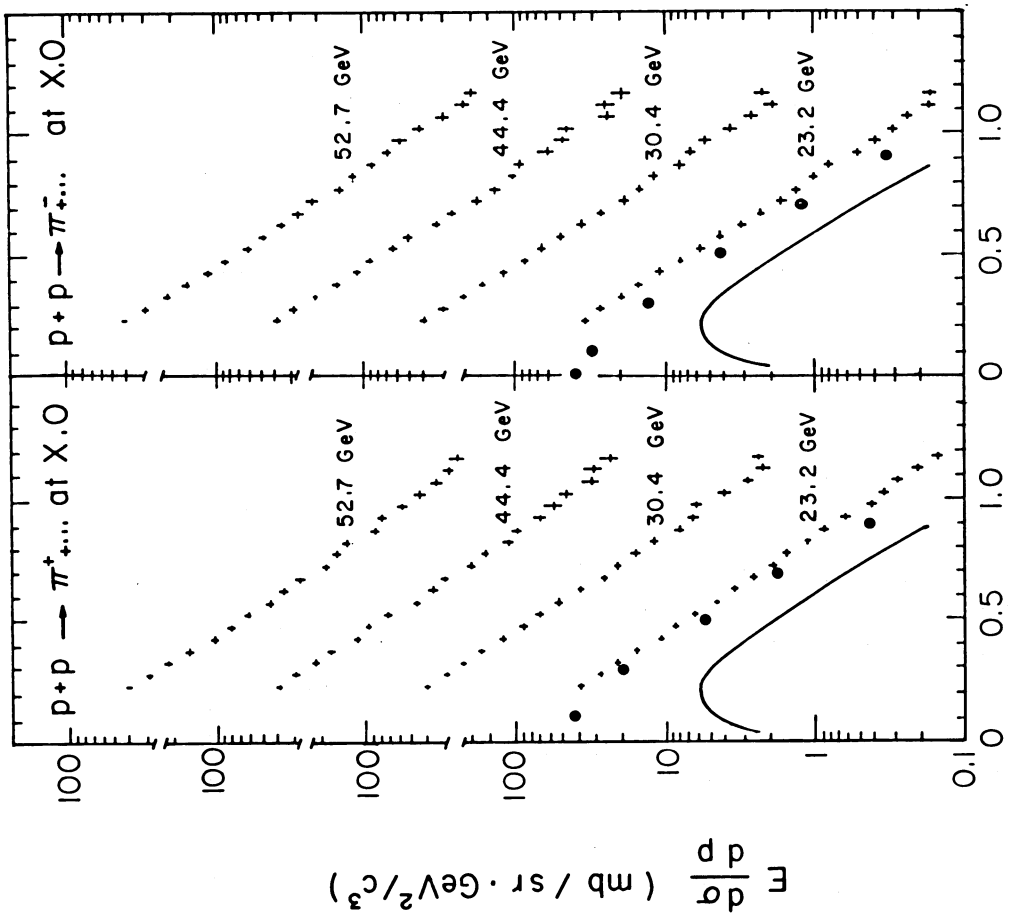
p+p → π±... at X.0
p+p → π±... at X.0
52.7 GeV
44.4 GeV
30.4 GeV
23.2 GeV
100
10
1
0.1
0
0.5
1.0
Pt (GeV)
E d σ/d p (mb / sr · GeV²/c³)

Fig. 8

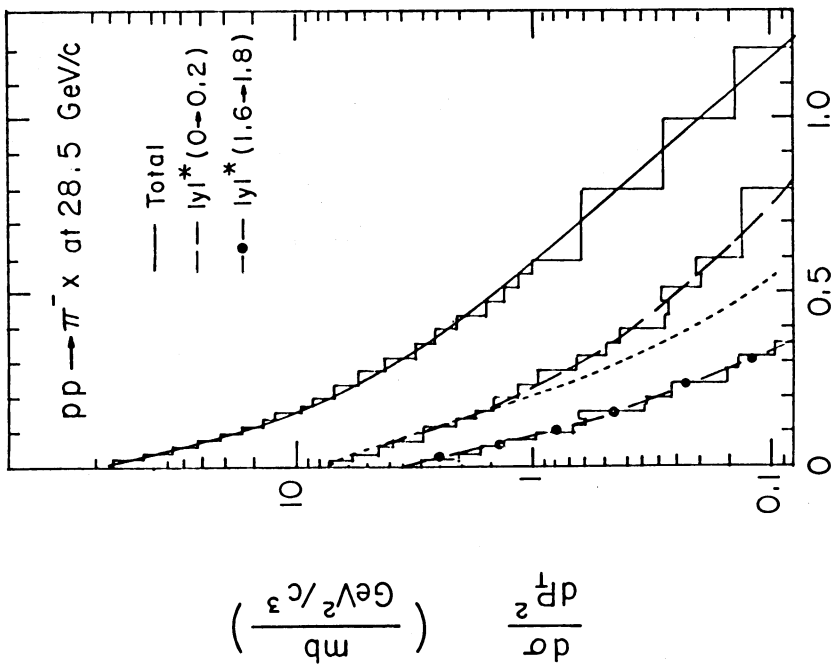
pp → π⁻ x at 28.5 GeV/c
Total
lyl*(0→0.2)
lyl*(1.6→1.8)
10
1
0.1
0
0.5
1.0
P²T (GeV/c)²
dσ/dP²T (mb/GeV²/c³)

Fig. 7

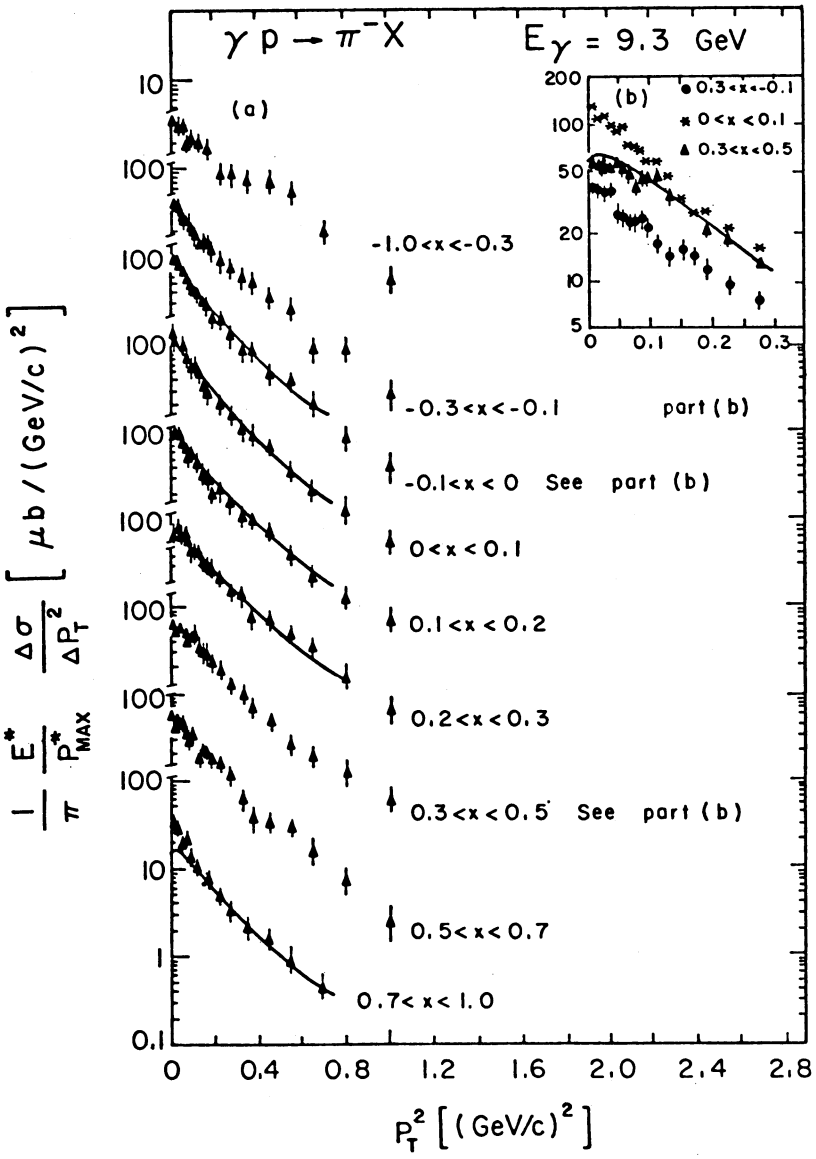
γ p → π⁻X
Eγ = 9.3 GeV
(a)
(b)
● 0.3<x<-0.1
✱ 0<x<0.1
▲ 0.3<x<0.5
-1.0<x<-0.3
-0.3<x<-0.1
part (b)
-0.1<x<0 See part (b)
0<x<0.1
0.1<x<0.2
0.2<x<0.3
0.3<x<0.5 See part (b)
0.5<x<0.7
0.7<x<1.0
1/π E*/P*MAX Δσ/ΔP²T [μb/(GeV/c)²]
P²T [(GeV/c)²]

Fig. 9